IASF/CNR
SEZIONE BOLOGNA
LFI Project System Team

Planck LFI

TITLE: **Optimisation of Edge Taper values for the 70 GHz LFI Feed Horns**

DOC. TYPE: TECHNICAL NOTE

PROJECT REF.: PL-LFI-PST-TN-039 **PAGE:** I of IV, 15

ISSUE/REV.: 1.0 **DATE:** April 2003

Prepared by	M. SANDRI F. VILLA C. BURIGANA LFI Project System Team M. BERSANELLI LFI Instrument Scientist	Date: Signature:	April 16th, 2003
Agreed by	C. BUTLER LFI Program Manager	Date: Signature:	April 16th, 2003
Approved by	N. MANDOLESI LFI Principal Investigator	Date: Signature:	April 16th, 2003

DISTRIBUTION LIST

Recipient	Company / Institute	E-mail address	Sent
M.BERSANELLI	Univ. Di Milano – Milano	bersanelli@uni.mi.astro.it	Yes
C.BURIGANA	IASF/CNR – Sezione di Bologna	burigana@bo.iasf.cnr.it	Yes
R.C.BUTLER	IASF/CNR – Sezione di Bologna	butler@bo.iasf.cnr.it	Yes
N.MANDOLESI	IASF/CNR – Sezione di Bologna	mandolesi@bo.iasf.cnr.it	Yes
A.MENNELLA	IASF/CNR – Sezione di Milano	daniele@mi.iasf.cnr.it	Yes
R.NESTI	CAISMI / CNR – Firenze	nesti@arcetri.astro.it	Yes
M.SANDRI	IASF/CNR – Sezione di Bologna	sandri@bo.iasf.cnr.it	Yes
F.VILLA	IASF/CNR – Sezione di Bologna	villa@bo.iasf.cnr.it	Yes
LFISPCC		lfispcc@bo.iasf.cnr.it	Yes

CHANGE RECORD

Issue	Date	Sheet	Description of Change	Release
1.0	16/04/03	All	First issue of document	==

TABLE OF CONTENTS

1 INTRODUCTION AND SCOPE

Scope of this technical note is to assess new edge taper requirements for the LFI 70 GHz channel. The aim is to improve the angular resolution of the LFI 70 GHz beams maintaining the Galactic Straylight Induced Noise (SIN) at a level lower than 3 μk peak to peak. For the baseline dual profiled corrugated feed horn #23 (PG26 – QM) the 4π antenna pattern has been computed using GRASP8 MrGTD and the corresponding Galactic SIN introduced by most relevant Galactic foreground components has been evaluated through astrophysical simulations. Then, the Edge Taper (ET) of this horn has been degraded in order to improve the angular resolution; the corresponding Galactic SIN has been extrapolated by the results of the detailed study carried out on the LFI #9 at 100 GHz. The same extrapolation has been assumed for the 70 GHz feed horns #22 and #21.

2 THE OPTICS

Components considered in optical simulations are the main PLANCK payload sub–systems: the dual reflector telescope, the first V–groove under the telescope, the telescope main baffle, and the focal plane unit where LFI feed horns are located.

Table 1 70 GHz LFI feed horn locations in the Focal Plane Unit (in the Reference Detector Plane coordinate system).

FH #	Location (X_{RDP},Y_{RDP},Z_{RDP}) [mm,mm,mm]			Orientation (θ,φ,ψ) [°,°,°]		
21	-101.86	17.69	20.86	11.38	-11.22	-21.29
22	-92.41	43.29	18.66	11.63	-28.71	-19.84
23	-76.38	69.37	14.54	11.93	-46.04	-18.26

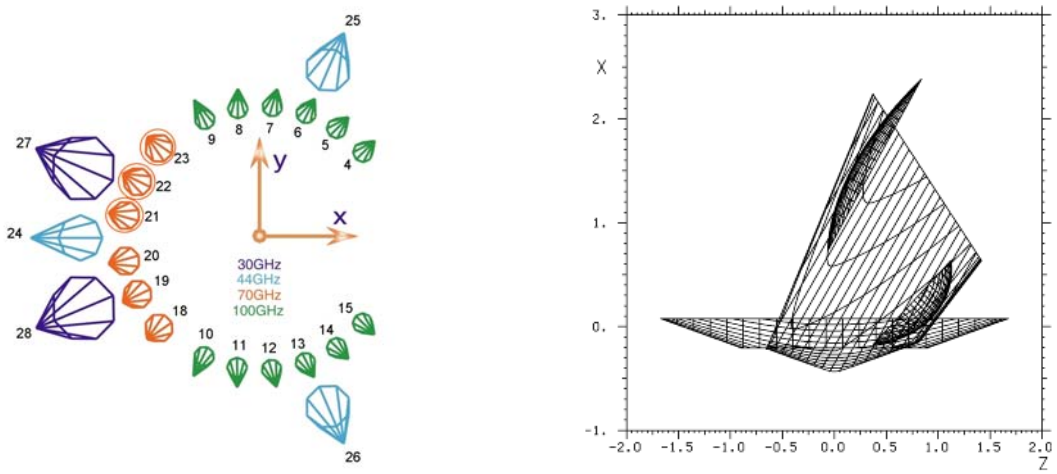

Figure 1 Planck/LFI Focal Plane Unit configuration. The 70 GHz LFI feed horns studied are marked with red circles. The axes are the X– and Y– axes of the Reference Detector Plane System (*left*). Telescope and shields geometry in $(XZ)_{TEL}$ plane (*right*).

3 STRAYLIGHT EVALUATION

The Galactic SIN for the baseline LFI #23 at 70 GHz has been evaluated through optical and astrophysical simulations as reported in 3.1, whereas the Galactic SIN of the tapered feed horns has been obtained combining the latter results with the knowledge acquired for the 100 GHz channel, as reported in 3.2.

3.1 GALACTIC SIN SIMULATION FOR THE BASELINE LFI #23

The Galactic SIN for the baseline LFI #23 (dual profiled corrugated feed horn – PG26) at 70 GHz has been evaluated using the antenna pattern computed with MrGTD. The pattern simulation is complete up to the 2nd order and contributions selected are those greater than –50 dBi in at least one point of the map. In the anti spillover region, where no ray has been found by the ray tracing procedure owing to the V-groove shade, the minimum of the map has been adopted.

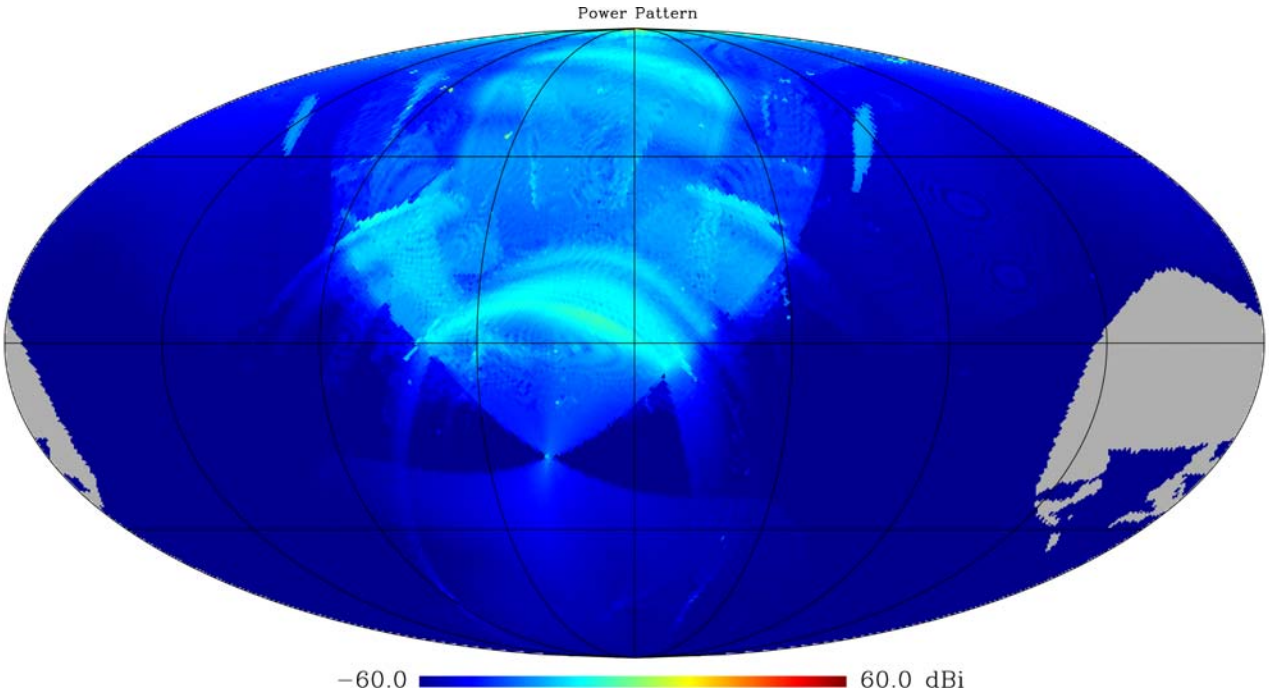

Figure 2 Full Pattern of the baseline LFI #23 at 70 GHz (power) computed in spherical cuts in which $-180° \le \vartheta \le 180°$ and $0° \le \varphi < 180°$, $\Delta\vartheta = 0.5°$ and $\Delta\varphi = 0.5°$. The boresight direction is at the top of the map. In the anti spillover region, around $\vartheta \sim 90°$ and $\varphi \sim 150°$, no ray coming from the source has been found and thus the total field is null.

Starting from this map and by assuming a realistic PLANCK scanning strategy, the Galactic Straylight Contamination introduced by most relevant Galactic foreground components (dust, diffuse free–free emission, diffuse synchrotron emission, and HII regions) has been evaluated, considering the latest MAP results. The resulting value is 0.85 μk (peak to peak) and 0.1 μk (RMS), in line with the LFI requirements for Straylight.

3.2 GALACTIC SIN PREDICTION FOR THE 70 GHZ FEEDS WITH DEGRADED EDGE TAPER

A correlation between Galactic SIN and Edge Taper as been found using the 100 GHz results reported in [1] and [2]. In Figure 3 and Figure 4 is shown the Straylight contamination (peak to peak and RMS, respectively) versus the Linear Edge Taper (LET), as computed for three different models of LFI #9 at 100 GHz. The solid line is the fitted curve (forcing the obvious zero crossing) of these three points, whose angular coefficient represents the Straylight degradation factor (194.417 μk peak to peak /LET and 21.51 μk RMS /LET) due to far side lobes and intermediate beam contamination (the dashed line represents the fitted curve of the three points due to intermediate beams, whereas the dotted line represents the fitted curve of the three points due to far sidelobes). Therefore, the extrapolated Straylight contamination at 70 GHz has been obtained as follows:

$$SC\ (\mu k, \text{peak to peak}) = 194.417 \times \Delta LET + 0.85$$

$$SC\ (\mu k, RMS) = 21.51 \times \Delta LET + 0.10$$

where ΔLET values considered are reported in Table 1, together with the corresponding ΔSC. The degradation is computed respect to the baseline LFI #23 with an ET equal to 20.5 dB @ 22° (i.e., 24.89 dB @ 24°).

Table 2 ET values considered and corresponding Straylight degradation computed using results of the 100 GHz fit.

ET (dB @ 24°)	ET (dB @ 22°)	ΔET (dB @ 24°)	ΔLET (@ 24°)	ΔSC ($\mu k_{\text{peak to peak}}$)	ΔSC (μk_{RMS})
20.64	17.00	4.25	0.00538149	1.04625	0.115756
20.04	16.50	4.85	0.00667519	1.29777	0.143583
19.43	16.00	5.46	0.00816302	1.58703	0.175587
19.00	15.65	5.89	0.00933544	1.81497	0.200805
18.22	15.00	6.67	0.01184190	2.30227	0.254720

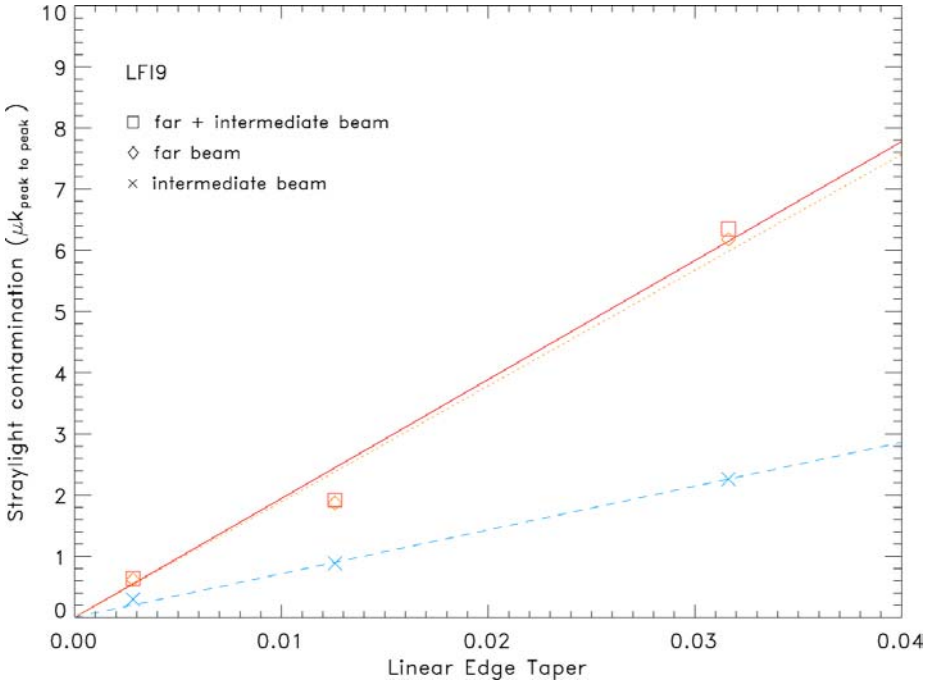

Figure 3 Correlation between Straylight Contamination (μk, peak to peak) and Edge Taper for the 100 GHz LFI feed horn #9.

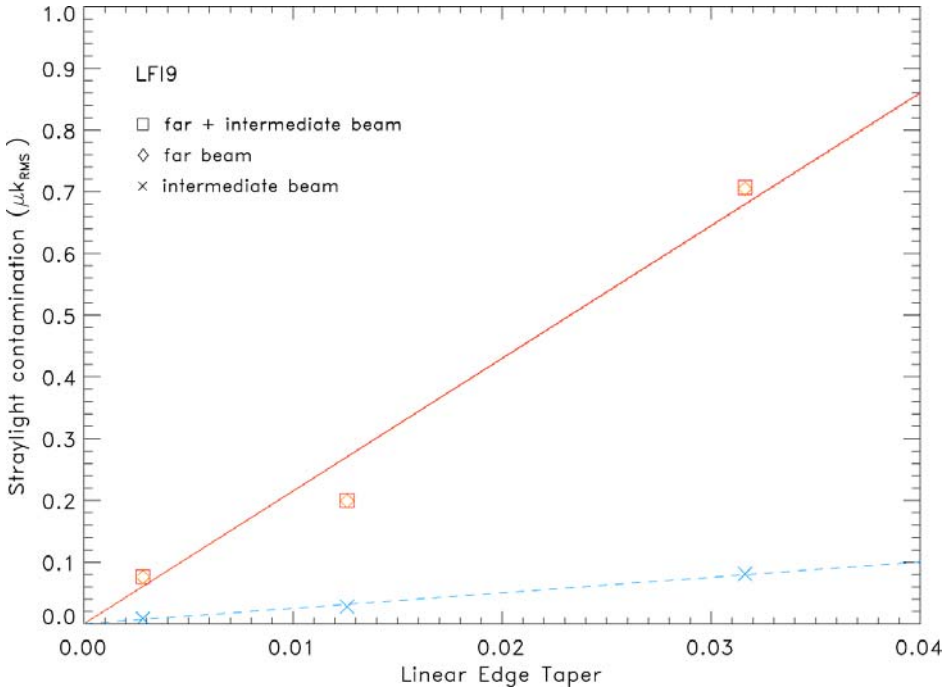

Figure 4 Correlation between Straylight Contamination (μk, RMS) and Edge Taper for the 100 GHz LFI feed horn #9.

4 FIELD DISTRIBUTION ON PRIMARY MIRROR

The contour plots of the amplitude field incident on the main reflector have been calculated for X–axis polarised Gaussian feeds with ET values reported in Table 2. The field distribution has been computed in a surface grid with 201 x 201 points. The axes of the contour plot are the X– and Y–axis in which the telescope is defined in GRASP software. The X– axis runs on the symmetry plane of the telescope while the Y– axis is on the asymmetry plane. The +Z direction, which corresponds to the main beam direction, is pointing orthogonal and then outward to the plane XY. As a consequence, the top edge of the main reflector is at X ~ 750 mm and Y~ 0 mm on the contour plot coordinate system. We used the Geometrical Optics on the sub reflector to calculate the total amplitude[1] of the field incident on the surface of the primary mirror, in the reference system of the main beam (the system has the Z– axis along the direction of the main beam peak and the XY–plane perpendicular to this direction).

4.1 FEED HORN #23

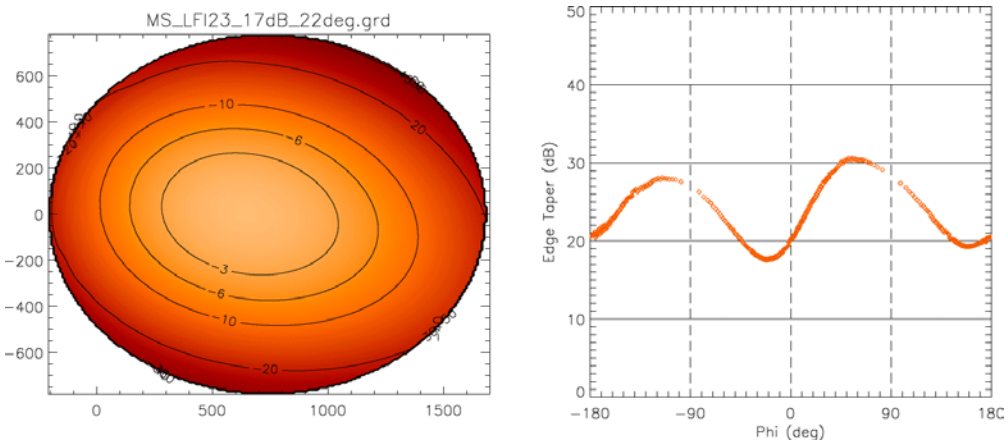

Figure 5 Field Distribution on the main reflector illuminated by the Gaussian feed #23 with an ET equal to 17dB@22°.

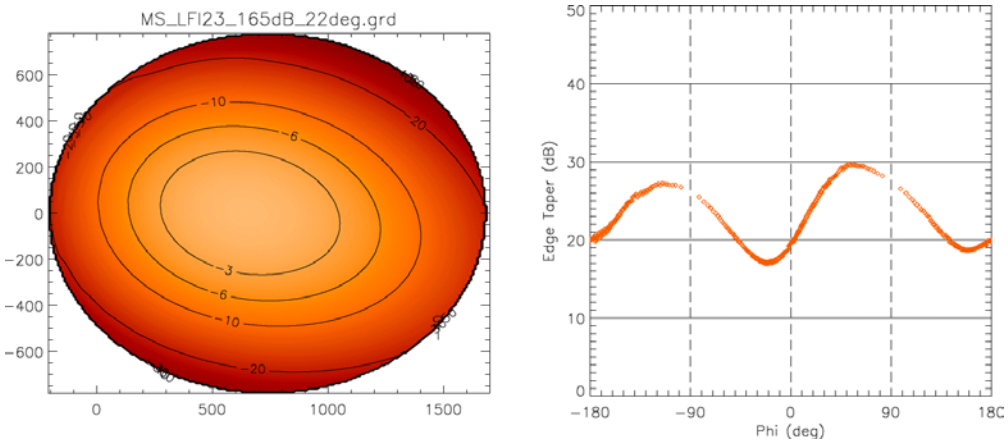

Figure 6 Field Distribution on the main reflector illuminated by the Gaussian feed #23 with an ET equal to 16.5dB@22°.

[1] The total amplitude in dB is defined as $E_{tot}^{dB} = 20 \cdot \log \sqrt{E_x^2 + E_y^2 + E_z^2}$

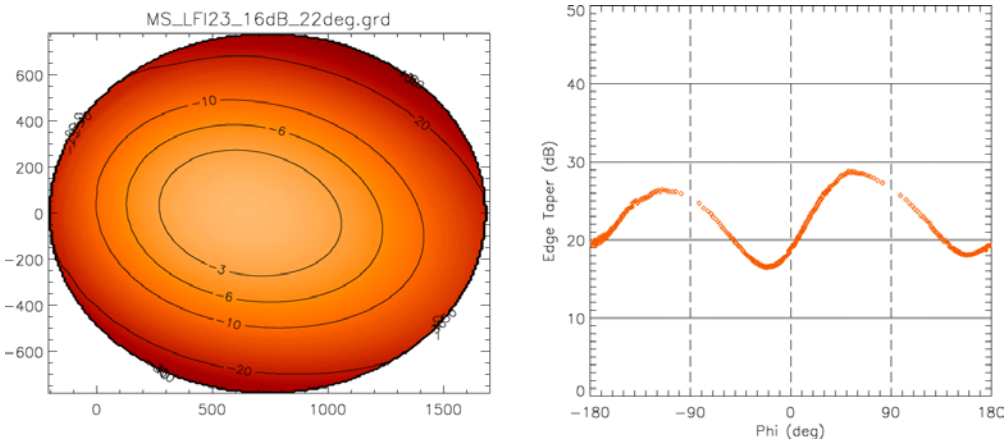

Figure 7 Field Distribution on the main reflector illuminated by the Gaussian feed #23 with an ET equal to 16dB@22°.

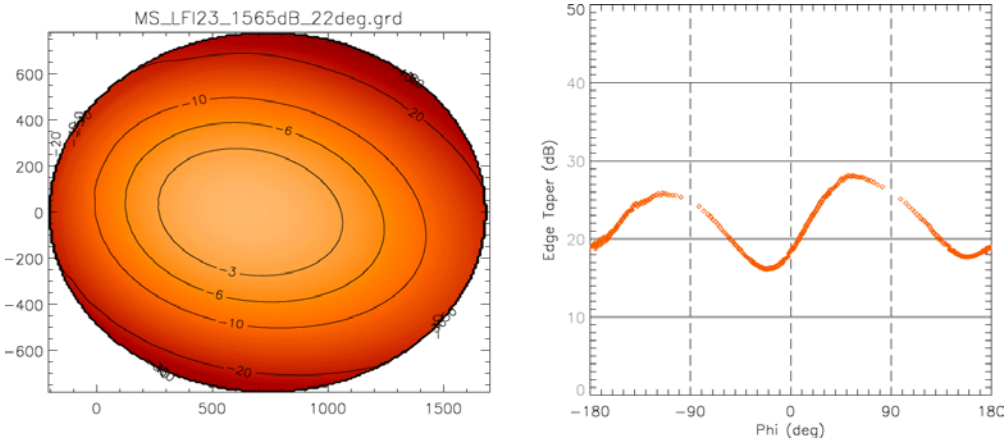

Figure 8 Field Distribution on the main reflector illuminated by the Gaussian feed #23 with an ET equal to 15.65dB@22°.

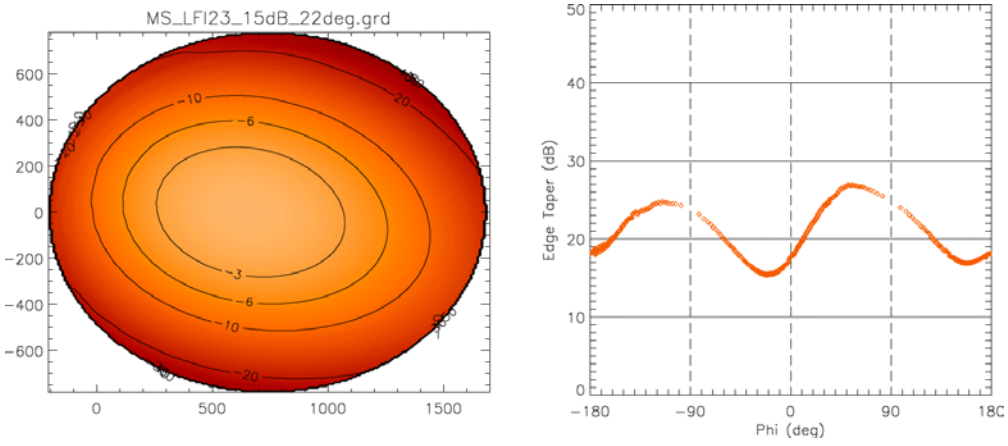

Figure 9 Field Distribution on the main reflector illuminated by the Gaussian feed #23 with an ET equal to 15dB@22°.

4.2 FEED HORN #22

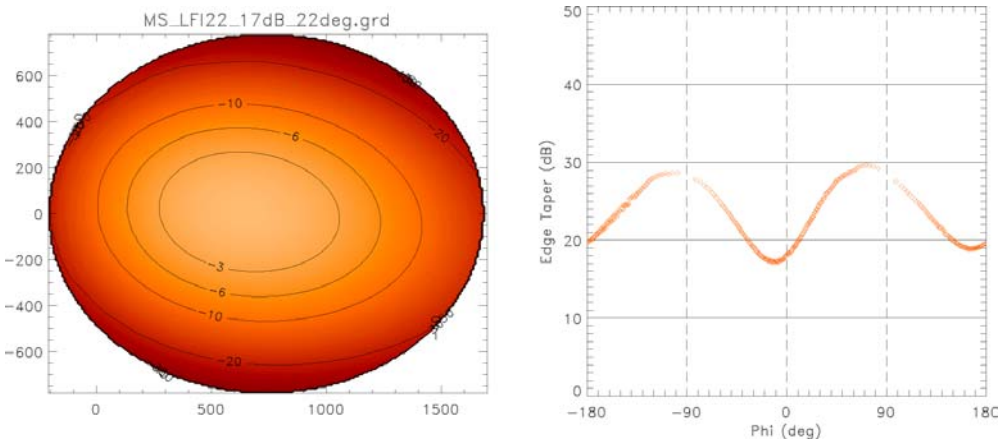

Figure 10 Field Distribution on the main reflector illuminated by the Gaussian feed #22 with an ET equal to 17dB@22°.

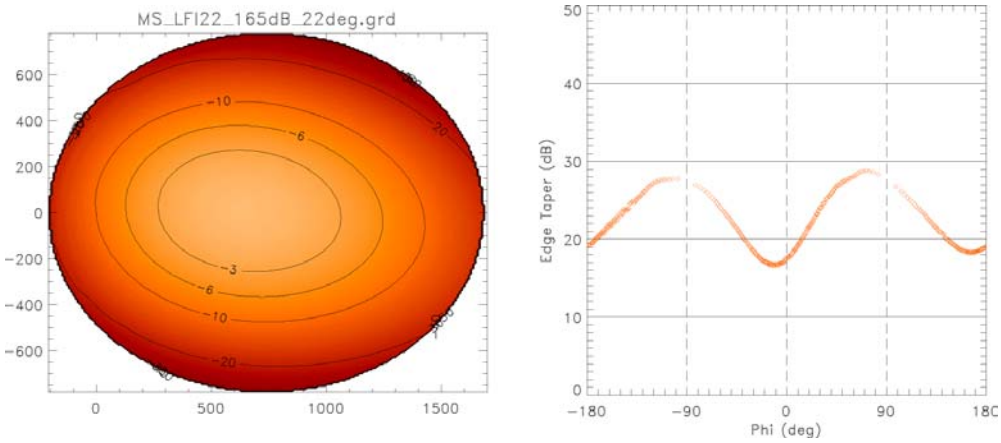

Figure 11 Field Distribution on the main reflector illuminated by the Gaussian feed #22 with an ET equal to 16.5dB@22°.

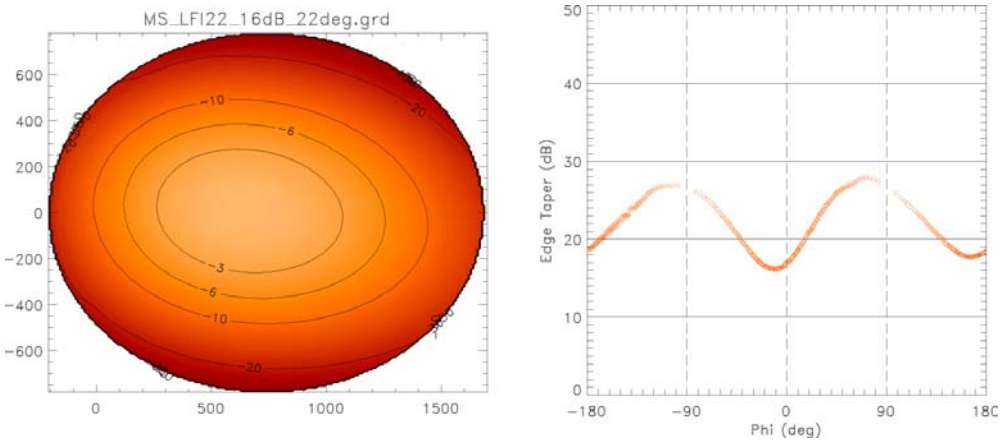

Figure 12 Field Distribution on the main reflector illuminated by the Gaussian feed #22 with an ET equal to 16dB@22°.

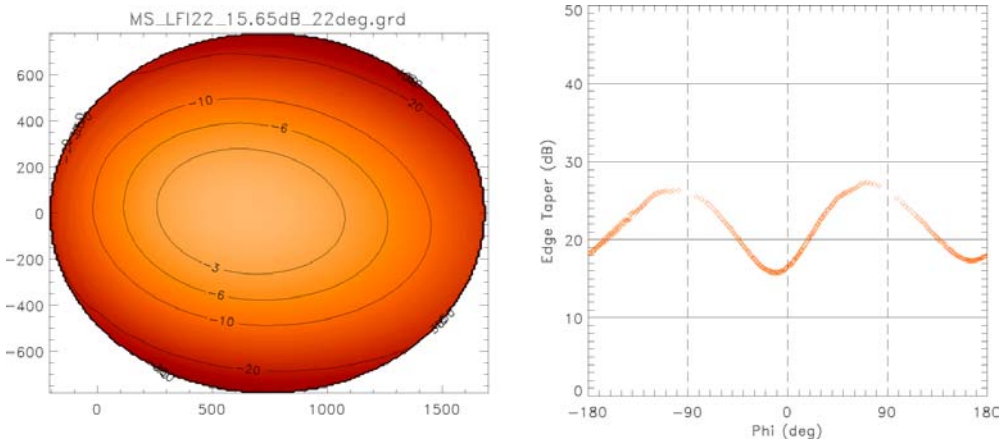

Figure 13 Field Distribution on the main reflector illuminated by the Gaussian feed #22 with an ET equal to 15.65dB@22°.

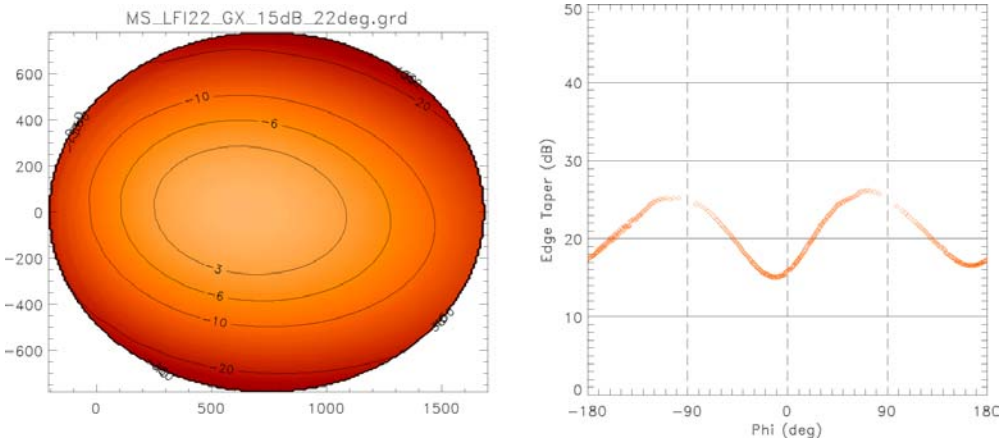

Figure 14 Field Distribution on the main reflector illuminated by the Gaussian feed #22 with an ET equal to 15dB@22°.

4.3 FEED HORN #21

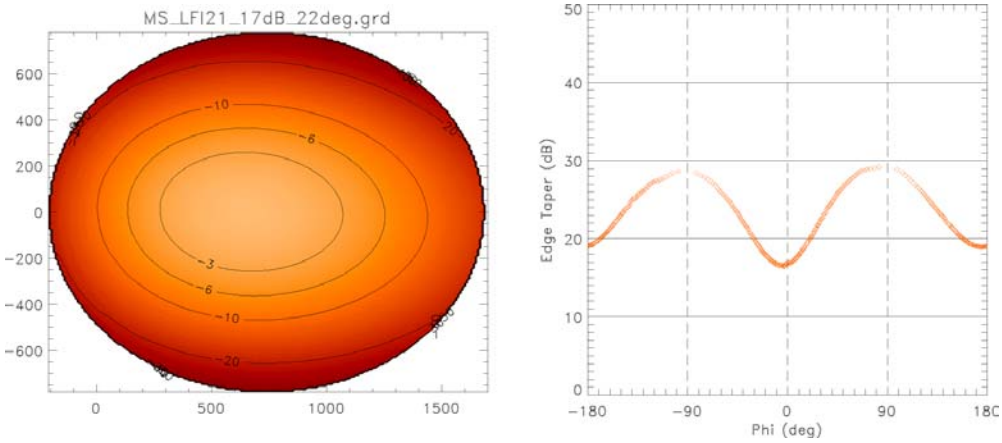

Figure 15 Field Distribution on the main reflector illuminated by the Gaussian feed #21 with an ET equal to 17dB@22°.

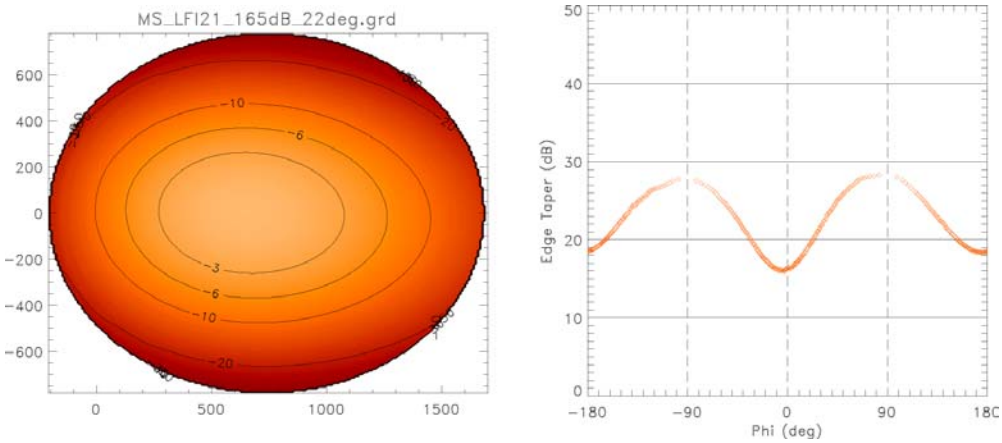

Figure 16 Field Distribution on the main reflector illuminated by the Gaussian feed #21 with an ET equal to 16.5dB@22°.

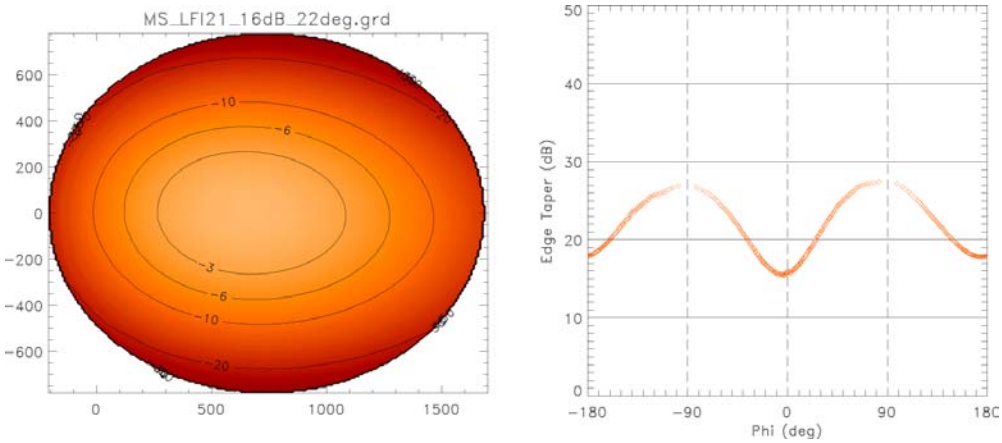

Figure 17 Field Distribution on the main reflector illuminated by the Gaussian feed #21 with an ET equal to 16dB@22°.

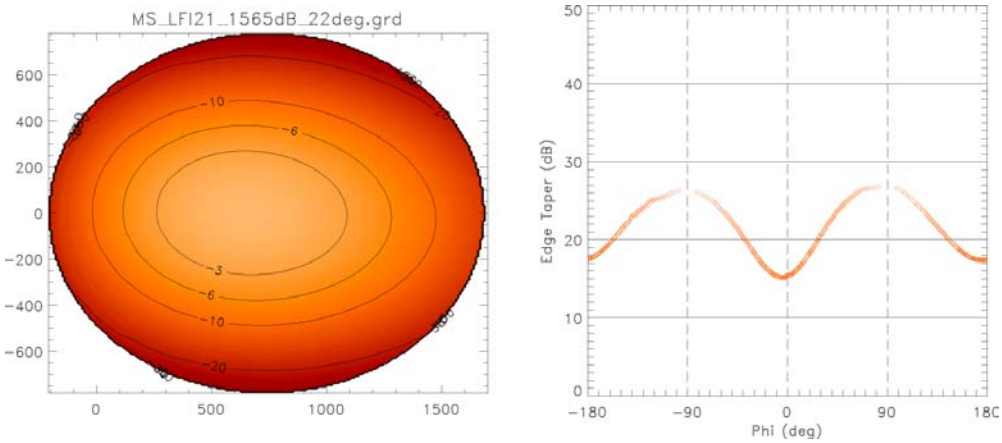

Figure 18 Field Distribution on the main reflector illuminated by the Gaussian feed #21 with an ET equal to 15.65dB@22°.

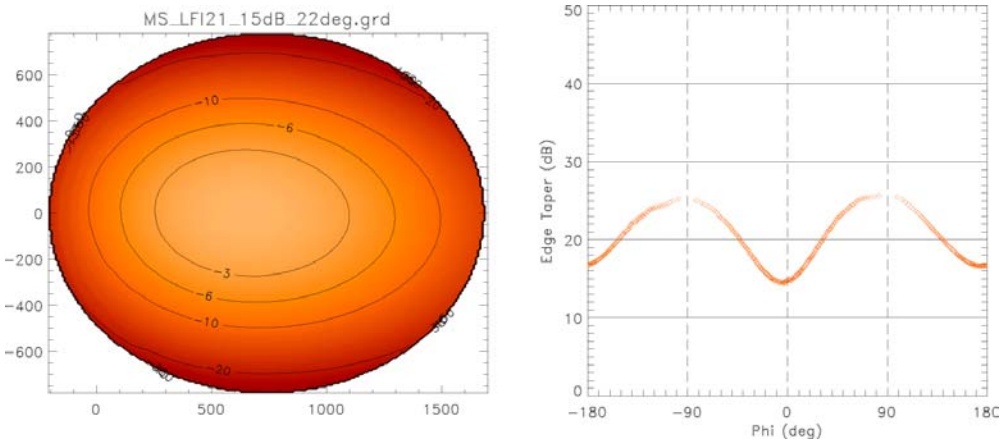

Figure 19 Field Distribution on the main reflector illuminated by the Gaussian feed #21 with an ET equal to 15dB@22°.

5 MAIN BEAMS

The main beam pattern has been simulated for each X– axis polarised Gaussian feeds with ET values reported in Table 2. The contour plots normalized at peak gain are shown in Figures from. The contour lines plotted are –3, –6, –10, –20, –30, –40, –50, –60 dB.

5.1 MAIN BEAM #23

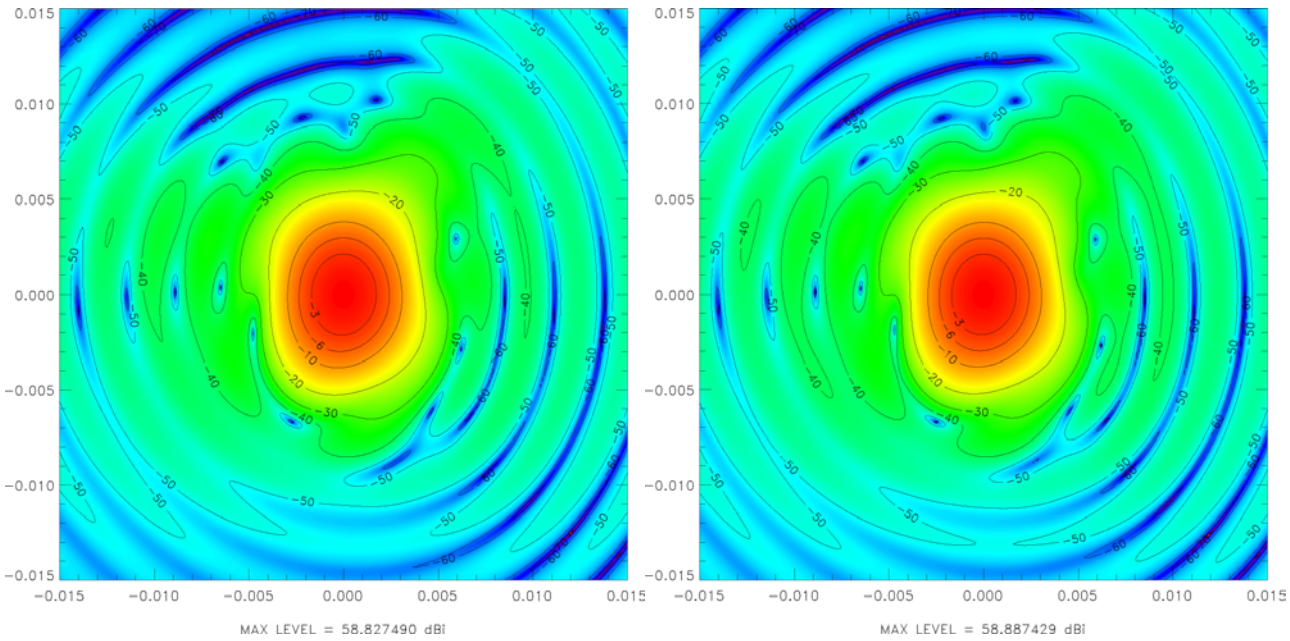

Figure 20 Co– polar component of Main Beam #23, ET 17dB@22° (left), and Main Beam #23, ET 16.5dB@22° (right).

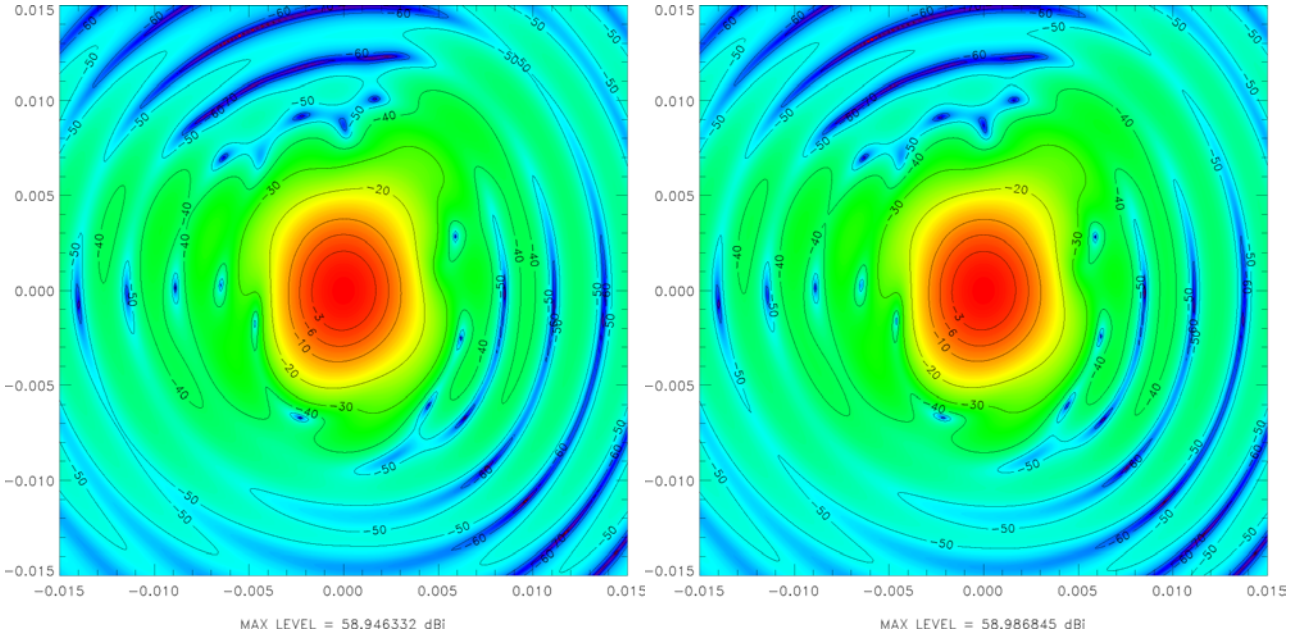

Figure 21 Co– polar component of Main Beam #23, ET 16dB@22° (*left*), and Main Beam #23, ET 15.65dB@22° (*right*).

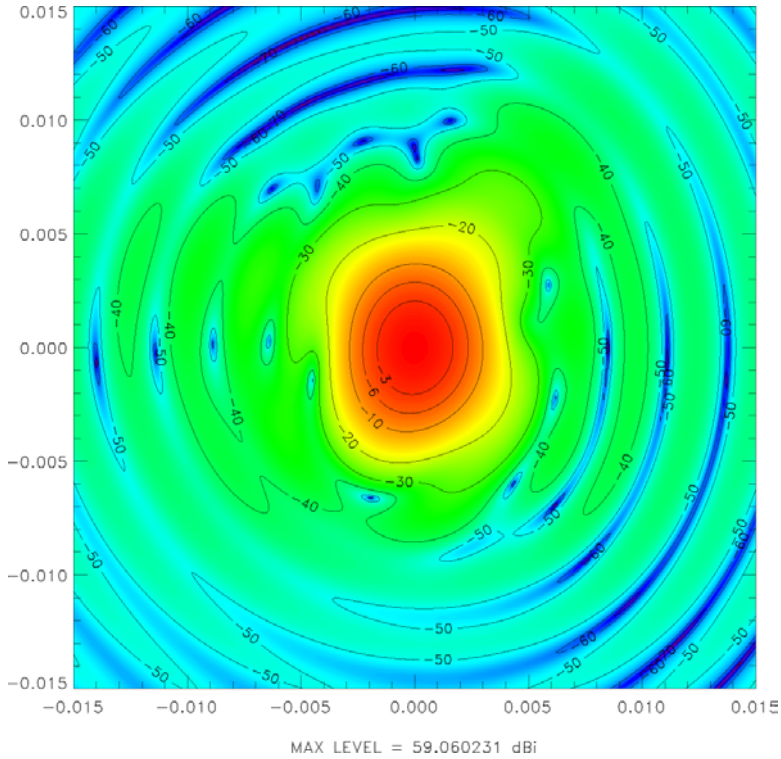

Figure 22 Co– polar component of Main Beam #23, ET 15dB@22°.

5.2 MAIN BEAM #22

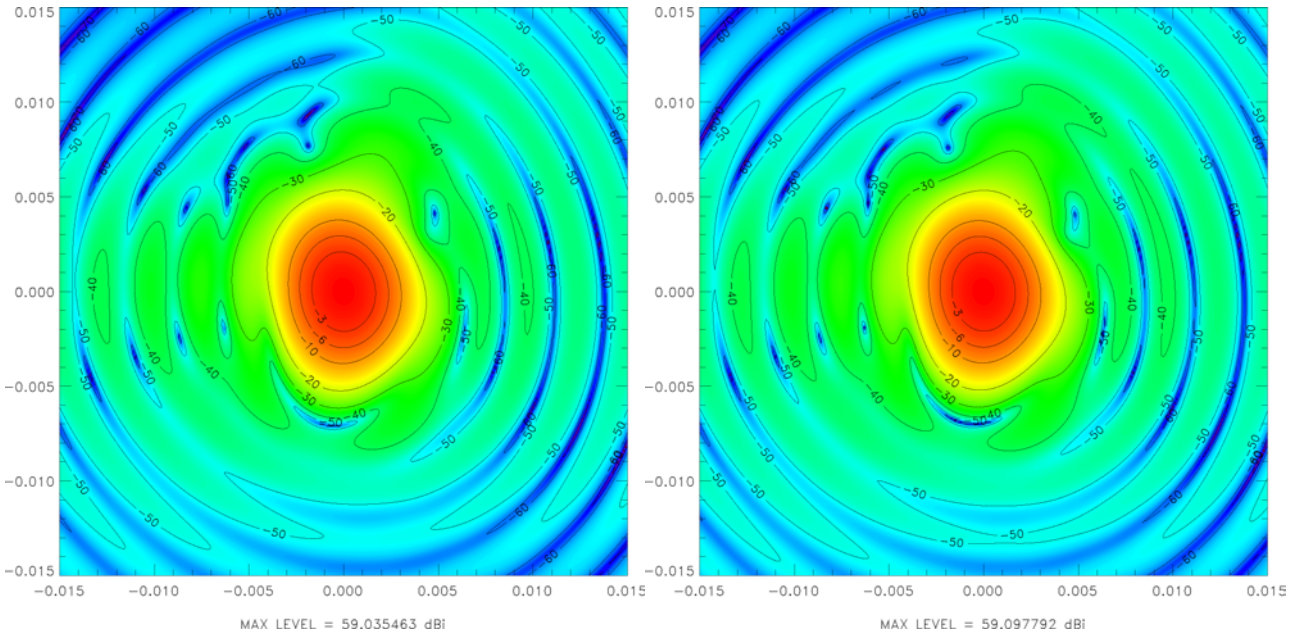

Figure 23 Co– polar component of Main Beam #22, ET 17dB@22° (left), and Main Beam #22, ET 16.5dB@22° (right).

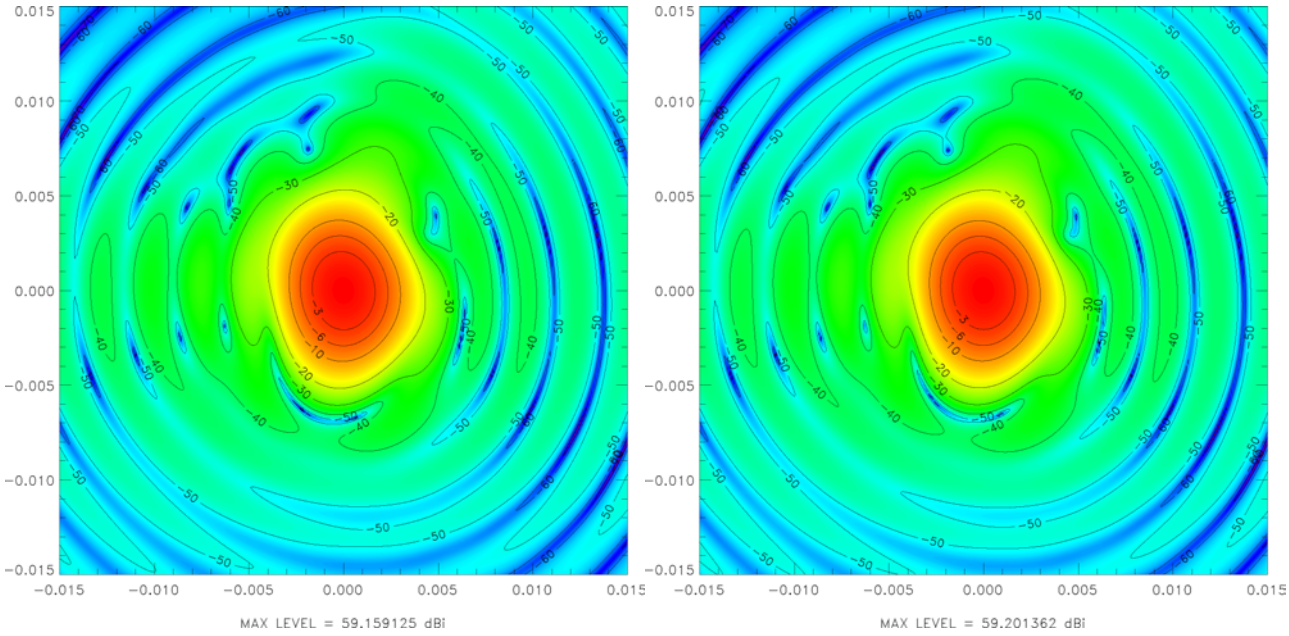

Figure 24 Co– polar component of Main Beam #22, ET 16dB@22° (left), and Main Beam #22, ET 15.65dB@22° (right).

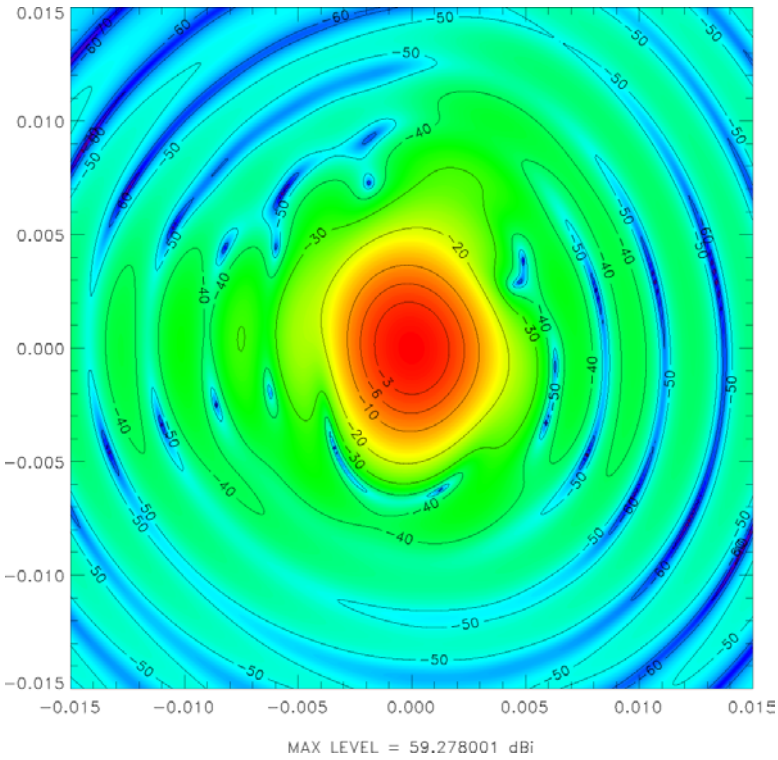

Figure 25 Co– polar component of Main Beam #22, ET 15dB@22°.

5.3 MAIN BEAM #21

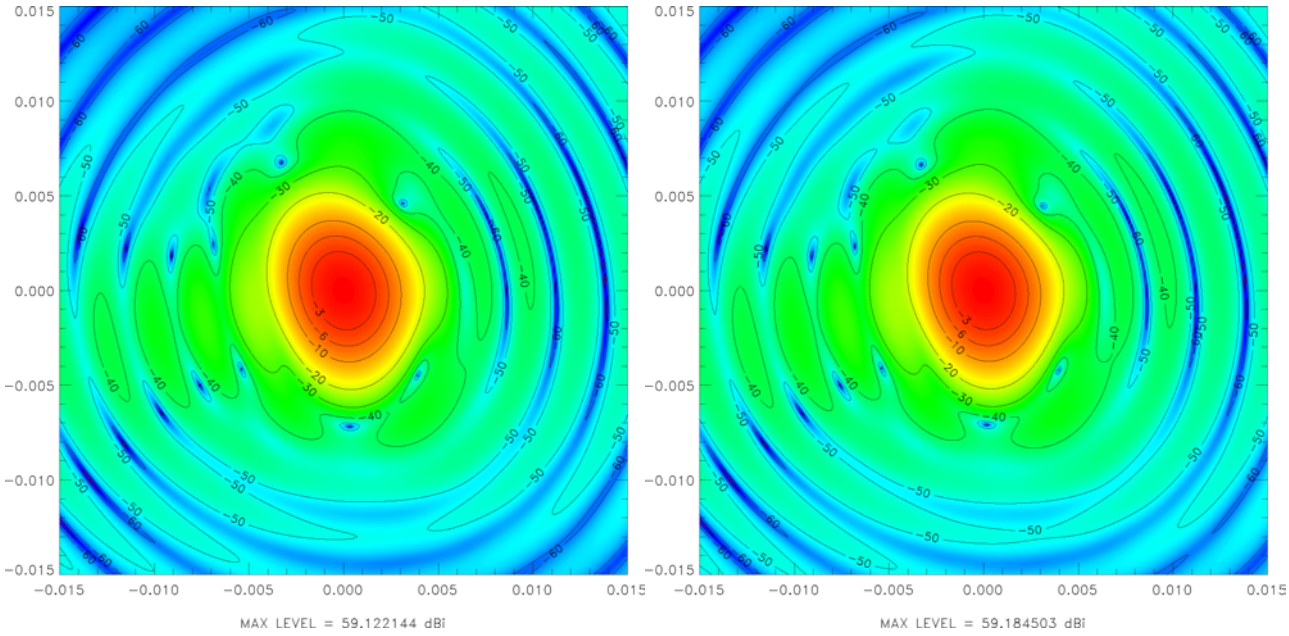

Figure 26 Co– polar component of Main Beam #21, ET 17dB@22° (left), and Main Beam #21, ET 16.5dB@22° (right).

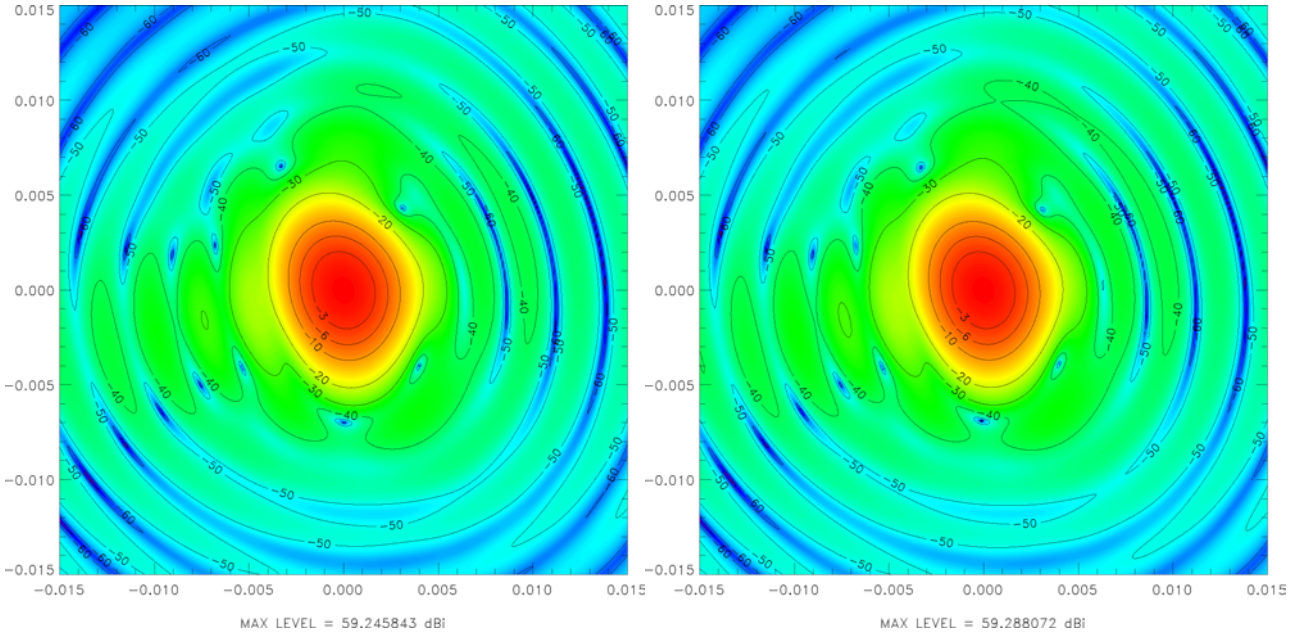

Figure 27 Co– polar component of Main Beam #21, ET 16dB@22° (left), and Main Beam #21, ET 15.65dB@22° (right).

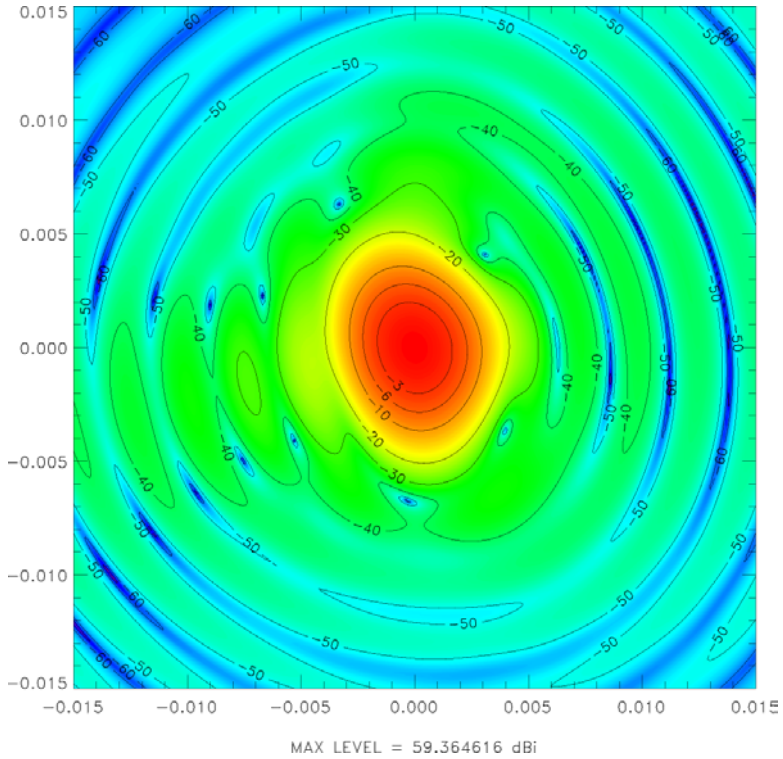

Figure 28 Co– polar component of Main Beam #21, ET 15dB@22°.

6 CONCLUSIONS

Feed	ET (dB @ 22°)	Dir (dBi)	FWHM (arcmin)			Straylight Contamination ($\mu k_{peak\ to\ peak}$)	Straylight Contamination (μk_{RMS})
			min	max	ave		
LFI 23	17.00	58.83	11.63	14.82	13.23	1.85	0.92
LFI 23	16.50	58.89	11.63	14.82	13.23	2.10	0.94
LFI 23	16.00	58.95	11.63	14.63	13.13	2.39	0.98
LFI 23	15.65	58.99	11.39	14.63	13.01	2.61	1.00
LFI 23	15.00	59.96	11.39	14.44	12.92	3.10	1.05
LFI 22	17.00	59.04	11.39	14.63	13.01	1.85	0.92
LFI 22	16.50	59.10	11.14	14.44	12.79	2.10	0.94
LFI 22	16.00	59.16	11.14	14.24	12.69	2.39	0.98
LFI 22	15.65	59.20	11.14	14.24	12.69	2.61	1.00
LFI 22	15.00	59.28	10.88	14.04	12.46	3.10	1.05
LFI 21	17.00	59.12	11.39	14.63	13.01	1.85	0.92
LFI 21	16.50	59.18	11.39	14.44	12.92	2.10	0.94
LFI 21	16.00	59.25	11.14	14.44	12.79	2.39	0.98
LFI 21	15.65	59.29	11.14	14.24	12.69	2.61	1.00
LFI 21	15.00	59.36	11.14	14.04	12.59	3.10	1.05

Table 3 Main Beam characteristics.

7 REFERENCES

1. M.Sandri, F.Villa, R.Nesti, C.Burigana, M.Bersanelli, N.Mandolesi, *Trade-off between angular resolution and straylight. Paper I* (to be submitted)

2. C.Burigana, M.Sandri, F.Villa, D.Maino, R.Paladini, C.Baccigalupi, M.Bersanelli, N.Mandolesi, *Trade-off between angular resolution and straylight. Paper II* (to be submitted)